PROCEEDINGS OF SCIENCE

Modeling CR electron propagation with PIERNIK & CRESP: simulations vs. observational data of NGC891

Mateusz Ogrodnik,[a,*] **Michal Hanasz,**[a] **Dominik Wóltański**[a] **and Artur Gawryszczak**[b]

[a] *Toruń Centre for Astronomy, Nicolaus Copernicus University, ul. Gagarina 11, 87-100 Toruń, Poland*

[b] *Nicolaus Copernicus Astronomical Center of the Polish Academy of Sciences, Bartycka 18, 00-716 Warsaw, Poland*

E-mail: mogrodnik@abs.umk.pl, mateusz.antoni.ogrodnik@gmail.com , mhanasz@umk.pl, wolt@umk.pl

Galactic outflows and extended non-thermal emission due to Comic Ray (CR) electrons have been observed in many edge-on galaxies in the radio range of electromagnetic radiation, allowing us to estimate the strength and vertical structure of the galactic magnetic field. We construct a global model of NGC891 based on the observational characteristics of this galaxy. We assume that on large scales, the dynamics of the magnetized ISM is driven by Cosmic Rays. We apply the coarse-grained momentum finite volume (CGMV), for solving the Fokker–Planck CR transport equation for CR electrons in "Cosmic Ray Energy SPectrum" (CRESP) module of PIERNIK MHD code to model CR propagation in this galaxy. The overall propagation of cosmic rays is described by the Fokker-Planck equation. The numerical model exhibits magnetic field amplification by CR-driven dynamo. We perform a parameter study of the system by varying the injection spectrum slope, the magnitude and momentum dependence of the CR electron diffusion coefficients and SFR. We take into account the advection, diffusion, and adiabatic changes as well as synchrotron and inverse-Compton losses. The spectrum of synchrotron radiation, polarization maps and spectral index maps reproduce the observed structures of the real edge-on galaxy very well. Comparison of different models suggests harder CRe^- injection spectra, higher conversion ratios of SN $\rightarrow$ CR energies (of 10–20%) and diffusion coefficients $\sim 9 \times 10^{28}\mathrm{cm}^2\mathrm{s}^{-1}$.

27th European Cosmic Ray Symposium - ECRS
25-29 July 2022
Nijmegen, the Netherlands

*Speaker

PoS(ECRS)131

1. Introduction

Radiofrequency continuum observations of distant galaxies often show halos and other structures extending far beyond features visible in the optical range, with emission extending farther out of the source at lower frequencies. This nonthermal radiation comes mainly from synchrotron emission of cosmic ray (CR) electrons [see, e.g. 1]. Radio observations of polarized radiation from edge-on galaxies show X-shaped structures in the polarised synchrotron emission [2, 3]. Phenomenological models [4] and MHD simulations [5, 6] indicate that these features may reflect the globally helical structure of large-scale magnetic fields in galactic halos [7]. The main questions related to this phenomenon concern: the formation mechanism and the global geometry and fine-scale structure of the magnetic field observed in X-shaped galaxies. Since radio observations only give a picture of polarised emission, the underlying magnetic field structure can only be deduced by comparison to plausible models, however, an ultimate verification of the models is inaccessible without a direct comparison of the observed emission of real galaxies against the polarized emission resulting from simulation models. But this is possible only if we have proper tools to simulate galactic propagation of CR electrons in a spectrally resolved manner. To reach this goal we have developed the Cosmic Ray Energy SPectrum (CRESP) algorithm [8], being a part of Piernik MHD code, to simulate the spectrally resolved population of CR electrons in MHD simulation runs of galaxies.

In this project we attempt to construct an MHD models of a nearby edge-on galaxy NGC 891, including CR protons driving the dynamics of the ISM together and spectrally CR electrons evolving in momentum dependent manner. Recent investigations of NGC891 feature low-frequency radio emission observations from LOFAR (Low-Frequency Array for radio astronomy) [9, 10]. The data presented include radio emission maps in various frequencies and resolutions with radiation intensity profiles, showing decreased emission range with increased frequency. Measured spectral index maps (α_n) indicate significant signs of flattening in the disk where fresh particles are supplied due to acceleration in SN remnants, with $\alpha_n \sim -0.37$ in the very centre and significant synchrotron ageing of particles in the halo, where $\alpha_n \sim -0.8$ was measured.

We aim to simulate a galactic disk similar to NGC 891 in which CR-driven dynamo process [see 5, and references therein] is imposed through the injection of CR protons, which couple dynamically with the thermal plasma. The CR-driven dynamics of the ISM constitutes an active background for the propagation of spectrally resolved CR electrons. We use Piernik MHD code and the CRESP module to simulate the momentum-dependent evolution of the CR electrons in NGC891, construct synthetic synchrotron emission maps, and compare observational data with numerical models.

2. Basic formulae

The numerical algorithm of the CRESP module has been designed to construct discretised solutions of the Fokker-Planck equation [e.g. 11]:

$$\frac{\partial f}{\partial t} = \underbrace{-\boldsymbol{u}\cdot\nabla f}_{\text{advection}} + \underbrace{\nabla(\kappa\nabla f)}_{\text{diffusion}} + \underbrace{\frac{1}{3}(\nabla\cdot\boldsymbol{u})p\frac{\partial f}{\partial p}}_{\text{adiabatic evolution}} \underbrace{\frac{1}{p^2}\frac{\partial}{\partial p}\left[p^2 b_l f + D_p\frac{\partial f}{\partial p}\right]}_{\text{synchrotron + IC and Fermi II}} + \underbrace{j}_{\text{sources}}. \tag{1}$$

where f is the CR distribution function, u is the thermal plasma velocity field, κ and D_p are the spatial and momentum space diffusion coefficients, b_l denotes the CR loss terms, j denotes the CR source terms (e.g. supernova remnants), t and p is time and the momentum coordinate.

Distribution function for CR e^- in momentum space p is approximated with power-law:

$$f(p) = f_{i-\frac{1}{2}} \left(\frac{p}{p_{i-\frac{1}{2}}} \right)^{-q_i}, \tag{2}$$

where $f_{i-1/2}$ – distribution function , q_i – slope indices. We parametrize diffusion coefficients for CR e^- using formula

$$\kappa(p_l)_{\parallel,\perp} = \kappa^{\mathrm{ref}}_{\parallel,\perp} \left(\frac{p_l c}{10\mathrm{GeV}} \right)^{\alpha_\kappa}. \tag{3}$$

where we usually assume $\kappa^{\mathrm{ref}}_{\parallel} = 3\text{–}9{\times}10^{28}$ cm^{2}s^{-1}, $\kappa_\perp \approx 1\%\kappa_\parallel$, and $\alpha_\kappa = 0.3$.

The Cosmic Ray Energy Spectrum Algorithm CRESP [8] is based on Miniati's COSMOCR code [12]. Equation (1), is added to the system of MHD equations and solved in 4D (physical + particle momentum space) [see 13, for a review on numerical techniques] CR distribution function is approximated with piece-wise power-law. The whole spectrum of CR particles can be described equivalently by two sets of discretised quantities:

$$(n_l, e_l) \Leftrightarrow (f_{i-\frac{1}{2}}, q_i), \qquad i = 1, N_{\mathrm{bin}}. \tag{4}$$

The spectrum spans in a range delimited by cutoff momenta (p_{lo}, p_{up}) variating in response to the energy loss and gain mechanisms. Parameter "e_{small}", representing a floor value of spectral energy density, is used to detect active spectrum bins processed in momentum space. The remaining bins containing CR electrons under the threshold value are subject only to advection-diffusion transport in space.

Simulation results are post-processed to construct Stokes parameters using stored information about CR particles' magnetic field, number and energy density data. Spectrum is recovered (relation 4) and used to compute number density $N_{\mathrm{CRe-}}(\gamma)$ corresponding to observed frequency ν and local **B**. Each cell contributes to synchrotron emissivity [14]:

$$J(\nu)d\nu \propto B^{\frac{1}{2}} \nu_{\mathrm{crit}}^{\frac{1}{2}} N_{\mathrm{CRe-}}(p/(mc))\, d\nu. \tag{5}$$

3. Setup

We perform a series of MHD simulation runs of a galaxy similar to NGC 891. We assume a fixed dark matter halo and simulate the evolution of the interstellar medium composed of gas, magnetic fields, cosmic ray protons in a single bin approximation and spectrally resolved cosmic ray electrons. The numerical setup of the galactic disk follows the paper [5], where we simulate CR propagation and magnetic field amplification in a disk galaxy. Here we study the dynamic effects of CRs on the evolution of magnetic fields in the model of the NGC 891 galaxy. We assume that the supernova rate is proportional to the star formation rate (SFR), which scales as a function of local gas density according to the Schmidt-Kennicutt-type law. We assume that 10% of the SN energy is converted to CR energy, out of which 1% is the energy of CR electrons. We assume that CR protons are dynamically coupled to the thermal plasma and neglect the thermal and kinetic energy output from supernovae. We assume that the source spectrum of CR electrons is a power law

distributed on the momentum grid of 14 bins. Assuming an under-equipartition initially toroidal magnetic field, we observe magnetic field amplification in the present simulations, as for the Milky Way model [5]. Using the CRESP algorithm, we study the evolution of the energy spectrum of the CR electron population and use it to create synthetic synchrotron radiation maps. We consider synchrotron, adiabatic and Inverse-Compton processes, advection, and diffusion transport for CR electrons. We use a static Eulerian nested grid with base resolution $96 \times 96 \times 64$ for the domain of physical sizes $115.2 \times 115.2 \times 76.8\,\mathrm{kpc}^3$, with three to four refinement levels. The smallest cell size for the highest resolution run is $(75\mathrm{pc})^3$.

4. Results

The synchrotron emission for one of the models in the edge-on perspective depicted in Figure 1 (top panel) shows the polarisation map superimposed on the total power (TP) map. The edge-on image of the simulated galaxy shows typical structures seen in observed galaxies [see, e.g. 15]. A galactic disk with a dominant horizontal magnetic field is visible. The polarization vectors indicate the presence of a vertical magnetic field in the galactic halo, particularly in the central region dominated by the veridical outflow of matter. In addition, for larger galactocentric radii, an "X" type structure is apparent. Since the fine-scale structures of the radio emission presented in the upper panel of Fig. 1. do not show very clearly, in the lower panel, we give a map for a one kpc thick layer perpendicular to the disk midplane. The bottom image shows filamentary structures of radio emission with characteristic sizes of 1 - 10 kpc.

A careful look at the radio map of the thin disk layer reveals the presence of magnetic field loops reminiscent of those formed by Parker instability. These loops result as the consequence of the cosmic rays' buoyancy. Due to the continuous production of cosmic rays in the supernova remnants, the buoyant flux tubes become stretched in the vertical direction. Therefore, the magnetic field loops tend to open towards the halo. The filaments visible in the TP map correlate with the polarisation vectors' direction.

Completing the picture of the radio emission intensity are the spectral index maps, shown in Figure 2, constructed between the 146 and 1421 MHz frequencies for the full depth of the computational domain and the central layer perpendicular to the observation direction. One can note that the central outflow, coinciding with open vertical magnetic fields, is populated by fresh electrons. The tangled magnetic structures further away from the centre are filled with spectrally aged electrons. Noticeable is the gradual ageing of synchrotron-emitting electrons along the open emission filaments.

Since we aim to compare the resulting spectral index maps with observational data for the galaxy NGC891, we show in Figure 3 the vertical profiles of spectral index obtained for a series of simulations and compared to the observational data published in [9]. Colour lines represent runs performed for different system parameter sets at t = 2Gyr. Analysing an extensive series of simulation runs, we find that some choices of parameters lead to results consistent with observational data. One of the most relevant parameters is the diffusion coefficient of CRs $K_{\parallel}$, scaling with momentum according to formula (3), where $\alpha_k = 0.3$.

Comparing the models with observations, we find a noticeable difference in that the simulated spectra are softer than the observed ones. There could be many reasons for the differences. First,

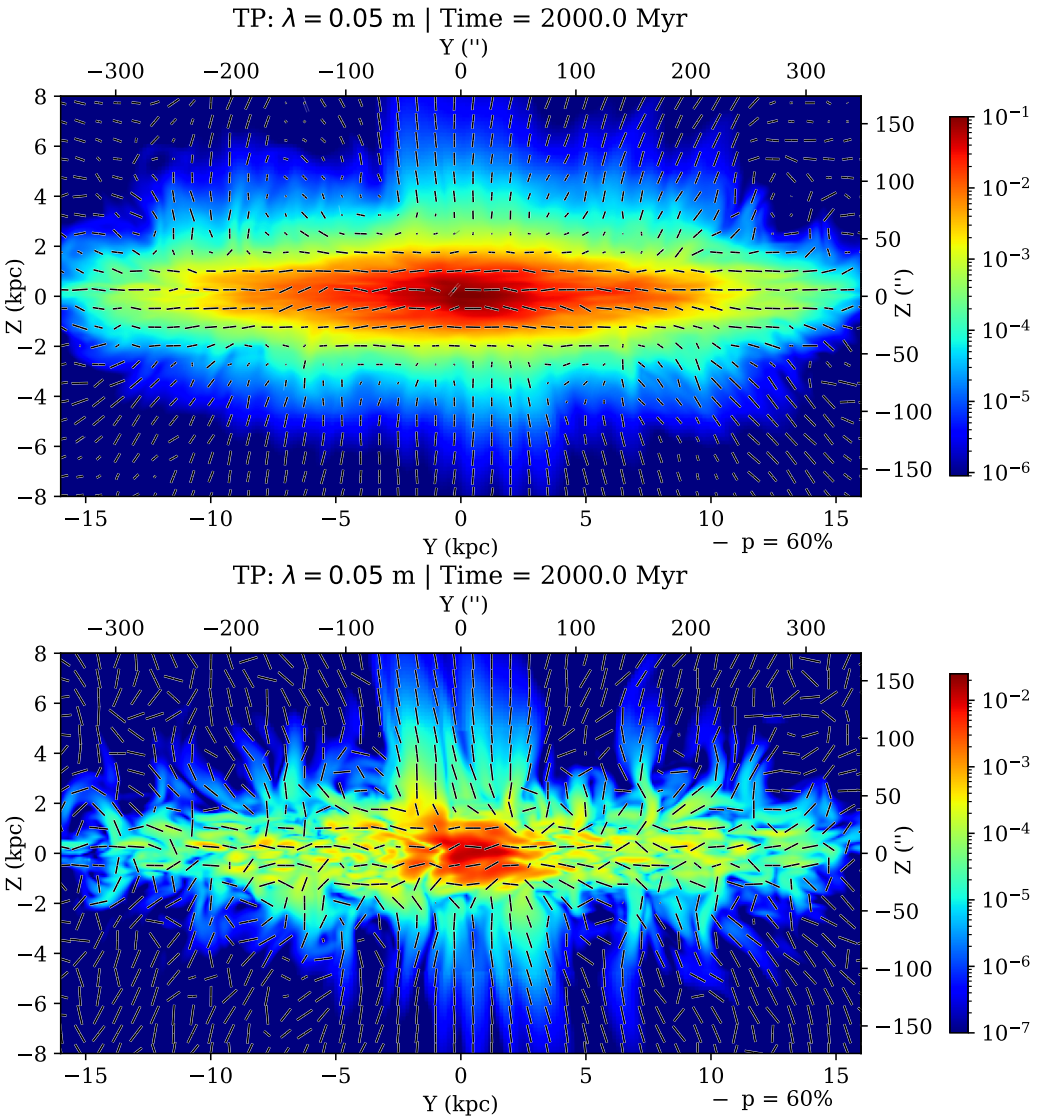

Figure 1: Total power (TP) maps with superposed polarization vectors representing radio emission at 5cm for epoch 2Gyr, integrated over the whole depth of computational domain (top) and a 1kpc-thin layer including galactic centre (bottom). The thin-layer image reveals the fine structure of magnetic loops and vertical magnetic filaments visible in synchrotron emission.

the magnetic field amplified by the CR-driven dynamo may be stronger than the actual magnetic field in NGC 891. The second reason may be the insufficient resolution of the computational grid of our simulations. If so, the magnetic field is subject to unphysical numerical reconnection. Consequently, oppositely polarised vertical field lines annihilate, so the effective diffusion of CR electrons in the direction perpendicular to the disk is slowed down. As a result, the electrons remain in the disk longer and are thus cooled more efficiently in the synchrotron process.

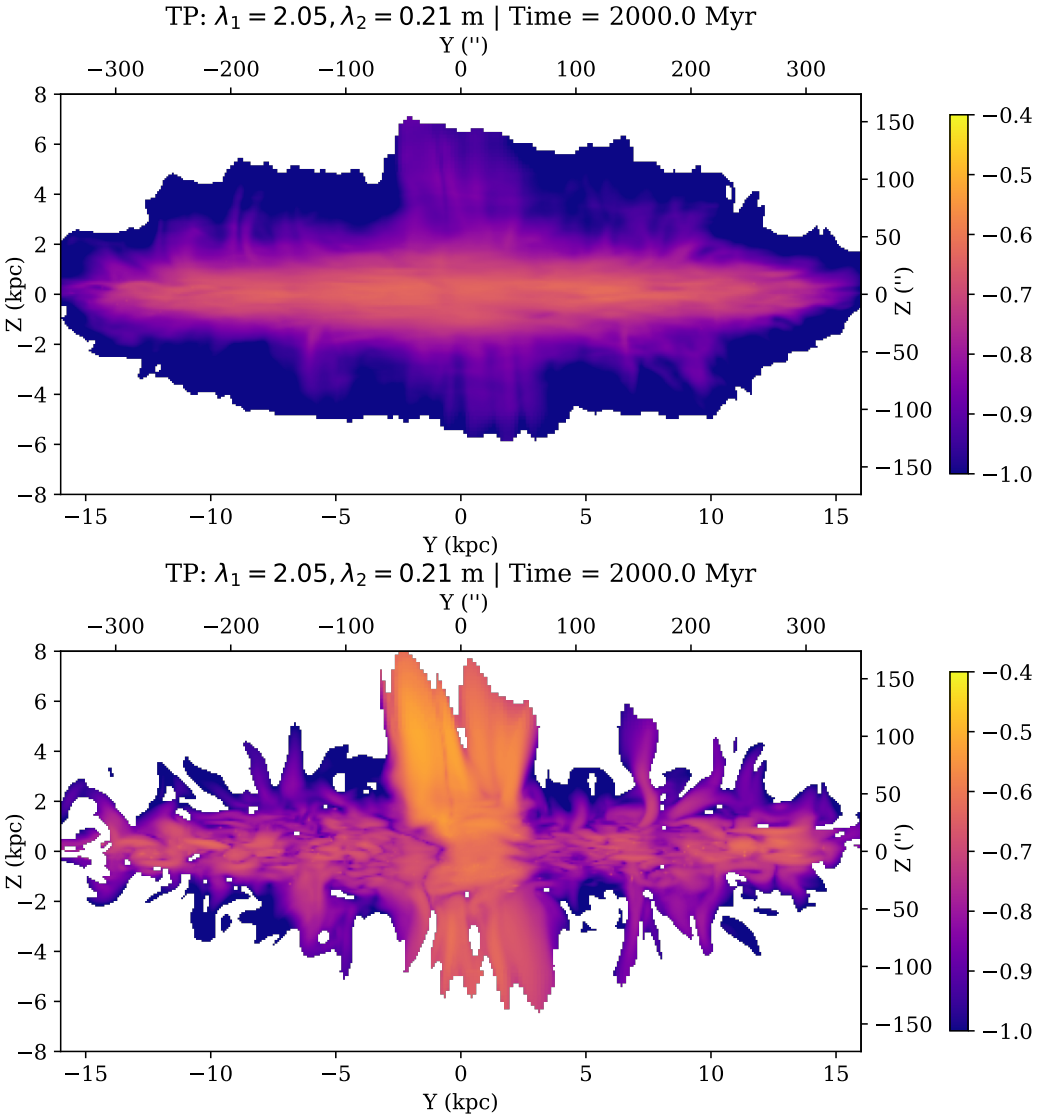

Figure 2: Spectral index (SI) maps between frequencies 146 & 1421 MHz at 2 Gyr for the synchrotron emission integrated over the whole depth of the computational domain (top), and a 1kpc-thin layer including galactic center (bottom). Synchrotron radio-maps display similar filamentary structures as the TP maps. Hard spectra (orange) represent fresh electrons, while soft spectra (dark blue) represent the electron population cooled down by synchrotron emission.

5. Conclusions

We find that models with the higher reference diffusion coefficient $K_{\parallel}^{\mathrm{ref}} = 9 \times 10^{28}\mathrm{cm}^2\mathrm{s}^{-1}$ at energies 10GeV (simulations B*, blue lines) agree better with the observational data than the other lines representing models with the lower diffusion coefficient ($3 \times 10^{28}\mathrm{cm}^2\mathrm{s}^{-1}$ (simulations A*, green and orange lines). Comparison of larger sets of models suggests that harder CRe^- injection spectra, higher conversion ratios of SN $\rightarrow$ CR energies (of 10–20%) and diffusion coefficients $\sim 9 \times 10^{28}\mathrm{cm}^2\mathrm{s}^{-1}$ fit better to observational data

Although matching simulation results to observational data is not perfect, we find that different

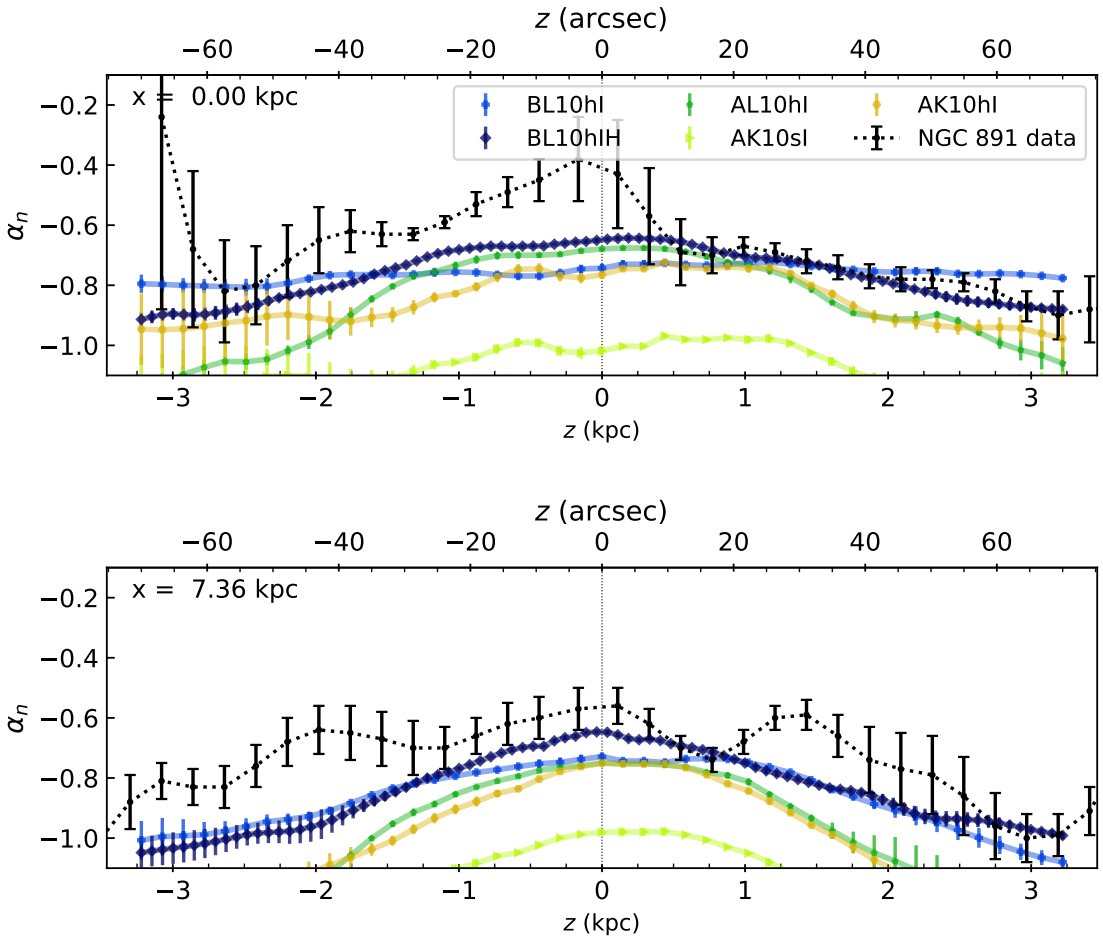

Figure 3: Vertical profiles of spectral index extracted from the full-depth SI maps similar to that presented in Figure 2 obtained for a series of simulation runs performed for different system parameter sets (colour lines) at t = 2Gyr. The black points with error bars represent observational data by Mulcahy et al. [9], courtesy of the authors. The upper panel shows SI profiles along vertical lines drawn through the galactic centre. The lower panel shows the profiles at the distance of 7.36kpc from the galactic centre.

cosmic ray propagation parameters lead to diversified results. This result is positive in that using spectral index and other synchrotron emission characteristics may help restrict parameters for both the ISM dynamics and CR propagation parameters in the future. Therefore, we conclude that MHD simulations of galaxies, including spectrally resolved cosmic ray transport and synchrotron emission, may become a powerful tool for ISM model diagnostics.

6. Acknowledgements

This work is supported by the Polish Ministry of Sciences and Higher Education and National Science Centre under OPUS-ST grant no. UMO-2015/19/B/ST9/02959. Computations were performed in Academic Informatics Centre TASK in Gdańsk and TCfA's Hydra cluster. We thank Volker Heesen for providing the spectral index data for the galaxy NGC 891.

7. References

[1] E. Orlando and A. Strong, *Galactic synchrotron emission with cosmic ray propagation models*, *MNRAS* **436** (2013) 2127 [1309.2947].

[2] M. Krause, *Magnetic Fields and Star Formation in Spiral Galaxies*, in *Revista Mexicana de Astronomia y Astrofisica Conference Series*, vol. 36 of *Revista Mexicana de Astronomia y Astrofisica, vol. 27*, pp. 25–29, Aug., 2009 [0806.2060].

[3] M. Soida, M. Krause, R.-J. Dettmar and M. Urbanik, *The large scale magnetic field structure of the spiral galaxy NGC 5775*, *A&A* **531** (2011) A127 [1105.5259].

[4] P. Terral and K. Ferrière, *Constraints from Faraday rotation on the magnetic field structure in the Galactic halo*, *A&A* **600** (2017) A29 [1611.10222].

[5] M. Hanasz, D. Wóltański and K. Kowalik, *Global Galactic Dynamo Driven by Cosmic Rays and Exploding Magnetized Stars*, *APJL* **706** (2009) L155 [0907.4891].

[6] D. Wóltański, *Cosmic-Ray-driven dynamo in spiral galaxies, PhD Thesis*, Nicolaus Copernicus University, Toruń (2014).

[7] V.N. Zirakashvili, D. Breitschwerdt, V.S. Ptuskin and H.J. Voelk, *Magnetohydrodynamic wind driven by cosmic rays in a rotating galaxy.*, *A&A* **311** (1996) 113.

[8] M.A. Ogrodnik, M. Hanasz and D. Wóltański, *Implementation of Cosmic Ray Energy Spectrum (CRESP) Algorithm in PIERNIK MHD Code. I. Spectrally Resolved Propagation of Cosmic Ray Electrons on Eulerian Grids*, *ApJSupp* **253** (2021) 18 [2009.06941].

[9] D.D. Mulcahy, A. Horneffer, R. Beck, M. Krause, P. Schmidt, A. Basu et al., *Investigation of the cosmic ray population and magnetic field strength in the halo of NGC 891*, *A&A* **615** (2018) A98 [1804.00752].

[10] M. Stein, V. Heesen, R.J. Dettmar, Y. Stein, M. Brüggen, R. Beck et al., *CHANG-ES. XXVI. Insights into cosmic-ray transport from radio halos in edge-on galaxies*, *A&A* **670** (2023) A158 [2210.07709].

[11] J. Skilling, *Cosmic ray streaming. III - Self-consistent solutions*, *MNRAS* **173** (1975) 255.

[12] F. Miniati, *COSMOCR: A numerical code for cosmic ray studies in computational cosmology*, *Computer Physics Communications* **141** (2001) 17 [astro-ph/0105447].

[13] M. Hanasz, A.W. Strong and P. Girichidis, *Simulations of cosmic ray propagation*, *Living Reviews in Computational Astrophysics* **7** (2021) 2 [2106.08426].

[14] M.S. Longair, *High Energy Astrophysics*, Cambridge, UK: Cambridge University Press (Feb., 2011).

[15] R. Beck, *Magnetic fields in spiral galaxies*, *A&AR* **24** (2015) 4 [1509.04522].